

## Fractional Lévy stable motion can model subdiffusive dynamics

Krzysztof Burnecki\* and Aleksander Weron†

*Hugo Steinhaus Center, Institute of Mathematics and Computer Science, Wrocław University of Technology,  
Wyspińskiego 27, 50-370 Wrocław, Poland*

(Received 23 April 2010; revised manuscript received 6 August 2010; published 31 August 2010)

We show in this paper that the sample (time average) mean-squared displacement (MSD) of the fractional Lévy  $\alpha$ -stable motion behaves very differently from the corresponding ensemble average (second moment). While the ensemble average MSD diverges for  $\alpha < 2$ , the sample MSD may exhibit either subdiffusion, normal diffusion, or superdiffusion. Thus,  $H$ -self-similar Lévy stable processes can model either a subdiffusive, diffusive or superdiffusive dynamics in the sense of sample MSD. We show that the character of the process is controlled by a sign of the memory parameter  $d = H - 1/\alpha$ . We also introduce a sample  $p$ -variation dynamics test which allows to distinguish between two models of subdiffusive dynamics. Finally, we illustrate a subdiffusive behavior of the fractional Lévy stable motion on biological data describing the motion of individual fluorescently labeled mRNA molecules inside live *E. coli* cells, but it may concern many other fields of contemporary experimental physics.

DOI: [10.1103/PhysRevE.82.021130](https://doi.org/10.1103/PhysRevE.82.021130)

PACS number(s): 05.40.Fb, 02.70.-c, 05.10.-a

### I. INTRODUCTION

Recent advances in nanotechnology have allowed to study biological processes on an unprecedented nanoscale molecule by molecule basis, opening the door to addressing many important biological problems [1–7]. A phenomenon observed in recent nanoscale single-molecule biophysics experiments is subdiffusion, which largely departs from the classical Brownian diffusion theory [8,9].

The issue of distinguishing between normal and anomalous diffusion, as such, concerns many fields of physics [10,11]. It is usually based on the analysis of the mean-squared displacement (MSD) of the diffusing particles. In the case of classical diffusion, the second moment is linear in time, whereas anomalous diffusion processes exhibit distinct deviations from this fundamental property:  $\langle x^2(t) \rangle \sim t^a$ , where for  $0 < a < 1$  is subdiffusive and for  $a > 1$  is superdiffusive [10]. The origin of anomalous dynamics in a given system is often unknown.

It is not always clear which model applies to a particular system [8,9,12], information which is essential when diffusion-controlled processes are considered. Therefore, determining the appropriate model is an important and timely problem; see [8,9,13] for discussion on the origins of anomaly in the case of intracellular diffusion.

The MSD can be obtained either by performing an average over an ensemble of particles, or by taking the temporal average over a single trajectory [14,15]. Recent advances in single-molecule spectroscopy enabled single particle tracking experiments following individual particle trajectories [9,13]. These require temporal moving averages.

In the literature, two popular stochastic models have been used to account for anomalous diffusion. The first one is the fractional Brownian motion (FBM) introduced by A.N. Kolmogorov in 1940 [16]. The second model of subdiffusion is

the continuous-time random walk (CTRW) and the corresponding fractional Fokker-Planck equation [10,17]. However, they do not exhaust all possible sources of anomalous diffusion. Another source could be random walks on fractal structures, percolation, etc. [10,18].

FBM is a generalization of the classical Brownian motion (BM). Most of its statistical properties are characterized by the Hurst exponent  $0 < H < 1$ . In particular, the MSD of FBM satisfies  $\langle x^2(t) \rangle \sim t^{2H}$ , thus for  $H < 1/2$  we obtain the subdiffusive dynamics, whereas for  $H > 1/2$  the superdiffusive one. For further properties of FBM and its applications to physics see [19–23].

For any  $0 < H < 1$ , FBM of index  $H$  (Hurst exponent) is the mean-zero Gaussian process  $B_H(t)$  with the following integral representation [16,20]:

$$B_H(t) = \int_{-\infty}^{\infty} \{(t-u)_+^{H-1/2} - (-u)_+^{H-1/2}\} dB(u), \quad (1)$$

where  $B(t)$  is a standard Brownian motion and  $(x)_+ = \max(x, 0)$ .

FBM is  $H$ -self-similar, namely for every  $c > 0$  we have  $B_H(ct) = c^H B_H(t)$  in distribution, and has stationary increments. It is the only Gaussian process satisfying these properties. For  $H > 1/2$ , the increments of the process are positively correlated and exhibit long-range dependence (long memory, persistence), whereas for  $H < 1/2$ , the increments of the process are negatively correlated and exhibit short-range dependence (short memory, antipersistence) [20]. For the second moment of the FBM we have  $\langle B_H^2(t) \rangle = \sigma^2 t^{2H}$ , where  $\sigma > 0$ , which for  $H < 1/2$  gives the subdiffusive dynamics and for  $H > 1/2$  the superdiffusive one.

It can be generalized to a fractional Lévy stable motion (FLSM) [19,20,24–26]:

$$Z_H^\alpha(t) = \int_{-\infty}^{\infty} \{(t-u)_+^d - (-u)_+^d\} dL_\alpha(u), \quad (2)$$

where  $L_\alpha(t)$  is a Lévy  $\alpha$ -stable motion (LSM),  $0 < \alpha \leq 2$ ,  $0 < H < 1$ , and  $d = H - 1/\alpha$ . The process is  $\alpha$ -stable (for  $\alpha = 2$  it

\*krzysztof.burnecki@pwr.wroc.pl

†aleksander.weron@pwr.wroc.pl

becomes a FBM),  $H$ -self-similar and has stationary increments. Analogously to the FBM case, we say the increments of the process exhibit positive (long-range) dependence if  $d > 0$  ( $H > 1/\alpha$ ), and negative dependence when  $d < 0$ , ( $H < 1/\alpha$ ) [25,26]. This is due to the behavior of the integrand in Eq. (2). Therefore, as in the Gaussian case, the parameter  $d$  controls sign of dependence.

We show in this paper that the time average MSD of FLSM behaves very differently from the corresponding ensemble average (second moment). This nonergodicity of FLSM is a timely subject since single-molecule experiments exhibit both anomalous kinetics and a large scatter of the time average MSD. While the ensemble average MSD diverges, the time average MSD may exhibit either subdiffusion, normal diffusion or superdiffusion (see Sec. II). Thus in experiment what seems subdiffusive from a single trajectory analysis could be in fact superdiffusive in the ensemble sense. The Gaussian case  $\alpha=2$  was treated already in [22].

We summarize here our main results which are threefold: (i) we propose in Sec. II to replace the MSD with a sample MSD and we show that a generalization of FBM to the Lévy stable law, namely, FLSM [19,20,24], provides a model for subdiffusive dynamics; (ii) following [7] we introduce in Section III a new  $p$ -variation dynamics test which allows to distinguish between FLSM and FBM and confirm that FLSM dynamics underlies the experimental observations independently of the size of the physical system; (iii) on the empirical side we illustrate in Sec. IV the subdiffusive phenomenon on Golding and Cox data [9], i.e., we check self-similarity of the data, estimate the Hurst exponent  $H$  and analyze the distribution of increments applying various statistical tests to find that the underlying distribution is Lévy stable with  $\alpha = 1.85$ .

## II. SAMPLE MSD

Let  $\{X_i, i=0, \dots, N\}$  be a sample of length  $N+1$ . We denote by  $\{Y_i = X_i - X_{i-1}, i=1, \dots, N\}$  its increment process. We introduce the sample MSD,

$$M_N(\tau) = \frac{1}{N-\tau+1} \sum_{k=0}^{N-\tau} (X_{k+\tau} - X_k)^2. \quad (3)$$

The sample MSD is a time average MSD on a finite sample regarded as a function of difference  $\tau$  between observations. It is a random variable in contrast to the ensemble average which is deterministic.

If the sample comes from an  $H$ -self-similar Lévy  $\alpha$ -stable process with stationary increments, we show that for large  $N$

$$M_N(\tau) \sim \tau^{2d+1}, \quad (4)$$

where  $d = H - 1/\alpha$  and  $\sim$  means similarity in distribution.

If  $\alpha=2$ , then by the law of large numbers [27], for large  $N$  and small  $\tau$

$$M_N(\tau) \sim \tau^{2H} \langle Y_1^2 \rangle = \tau^{2(H-1/2)+1} \langle Y_1^2 \rangle = \tau^{2d+1} \langle Y_1^2 \rangle, \quad (5)$$

where  $d = H - 1/2$ .

For  $\alpha < 2$  we rewrite the sample MSD as

$$\frac{1}{N-\tau+1} \left\{ \sum_{k=0}^{N/\tau-1} (X_{(k+1)\tau} - X_{k\tau})^2 + \sum_{k=0}^{N/\tau-2} (X_{(k+1)\tau+1} - X_{k\tau+1})^2 + \dots + \sum_{k=0}^{N/\tau-2} (X_{(k+1)\tau+\tau-1} - X_{k\tau+\tau-1})^2 \right\}. \quad (6)$$

By [28], for large  $N/\tau$ ,

$$\begin{aligned} M_N(\tau) &\sim \frac{1}{N-\tau+1} \left\{ \tau^{2H} (N/\tau)^{2/\alpha} S_{\alpha/2} \right. \\ &\quad \left. + (\tau-1) \tau^{2H} (N/\tau-1)^{2/\alpha} S_{\alpha/2} \right\} \sim \tau^{2H} \tau (N/\tau)^{2/\alpha} S_{\alpha/2} \\ &= C(N) \tau^{2(H-1/\alpha)+1} S_{\alpha/2} = C(N) \tau^{2d+1} S_{\alpha/2}, \end{aligned} \quad (7)$$

where  $C(N) = N^{2/\alpha}$ ,  $d = H - 1/\alpha$  and  $S_{\alpha/2}$  is a Lévy  $\alpha/2$ -stable random variable with the skewness parameter  $\beta=1$ . Therefore,  $S_{\alpha/2}$  is only one-sided.

Applying Eq. (4), we estimated memory parameter  $d$  for generated FLSM's in both cases of sub- and superdiffusion. The results are presented in Fig. 1 in the form of the so-called box plots [29,30]. The simulated samples are of length  $2^{10}$  which corresponds to longer trajectories of the experimental data [9]. The box plot produces a box and whisker plot for each value of  $d$ . The box has lines at the lower quartile, median, and upper quartile values. The whiskers are lines extending from each end of the box to show the extent of the rest of the data. Outliers are data with values beyond the ends of the whiskers. We can see that the medians of estimated  $d$  coincide well with the theoretical values.

In particular, for a FBM we obtain the well-known result that  $M_N(\tau) \sim \tau^{2H}$ , and for both BM and LSM we arrive at the diffusion case, namely  $M_N(\tau) \sim \tau$  since  $d=0$ , see also [31].

As a consequence, we see that the memory parameter  $d$  controls the type of anomalous diffusion. If  $d < 0$  ( $H < 1/\alpha$ ), so in the negative dependence case, the process follows the subdiffusive dynamics, if  $d > 0$  ( $H > 1/\alpha$ ), the character of the process changes to superdiffusive. What is even more amazing, it appears that Lévy  $\alpha$ -stable processes for  $\alpha < 2$  can serve both as examples of subdiffusion and superdiffusion. This is illustrated in Fig. 2. The subdiffusion pattern arises when the dependence is negative, so possible large positive jumps are quickly compensated by large negative jumps, and on average the process travels shorter distances than the light-tailed Brownian motion.

Most physical systems are of finite size and the observation time is possibly limited. In all such cases, boundary effects might become important for MSD, see e.g., [32,33]. However, it has been recently demonstrated in [34] that a finite size effect has no impact on  $p$ -variation methodology. This makes the use of  $p$ -variation test in finite size systems important.

## III. SAMPLE $p$ -VARIATION DYNAMICS TEST

Let us now discuss the idea of  $p$ -variation,  $p > 0$ . The concept of  $p$ -variation generalizes the well-known notions of total or quadratic variations, which have found applications

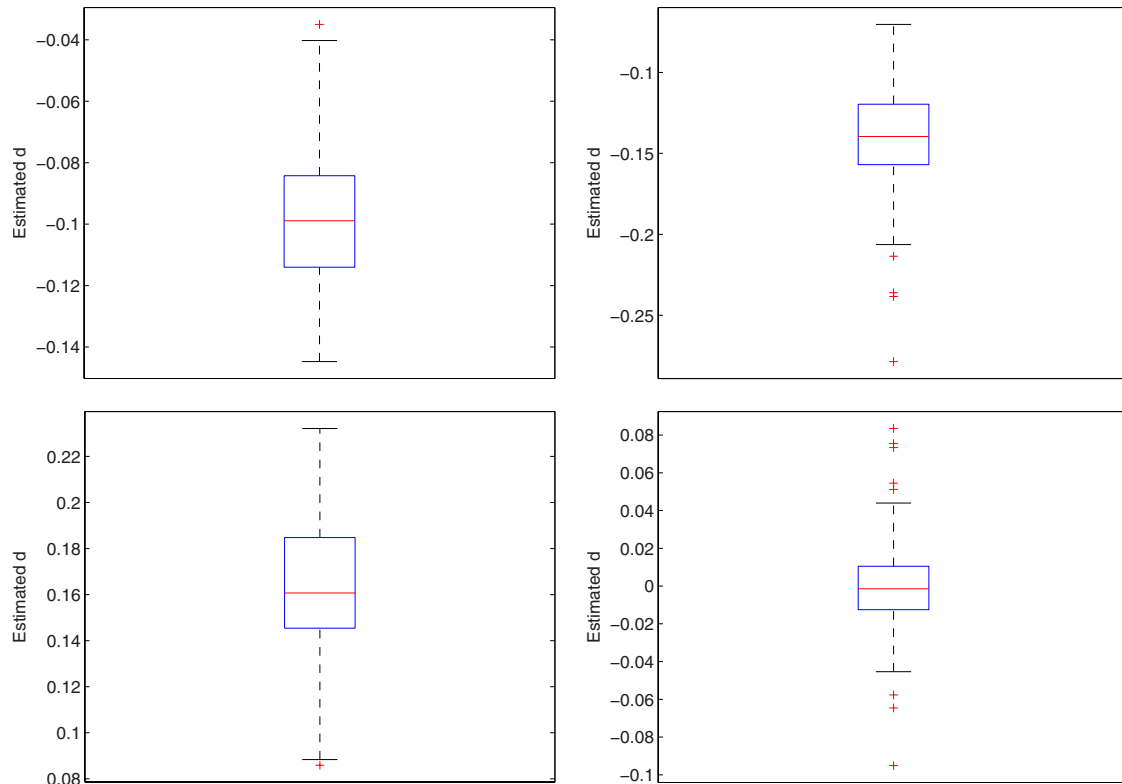


FIG. 1. (Color online) Box plots of the sample MSD estimates of the memory parameter  $d$  obtained via 1000 simulated trajectories of FLSM of length  $2^{10}$  with different  $H$ 's and  $\alpha$ 's. (Top left panel)  $H=0.4$ ,  $\alpha=2$  (FBM),  $d=H-1/\alpha=-0.1$ , (top right panel)  $H=0.4$ ,  $\alpha=1.85$   $d\sim-0.1405$ , (bottom left panel)  $H=0.7$ ,  $\alpha=1.85$ ,  $d\sim0.1595$ , (bottom right panel)  $H=0.7$ ,  $\alpha=1/0.7$  (LM),  $d=0$ .

in various areas of physics [7,18], mathematics and engineering [35]. Let  $X(t)$  be a stochastic process analyzed on the time interval  $[0, T]$ . Then, the  $p$ -variation of  $X(t)$  is defined as the limit of sum of increments of  $X(t)$  taken to the  $p$ -th power over all partitions  $P$  of the interval  $[0, T]$ , when the mesh of the partitions goes to zero. When  $p=1$  it reduces to the total variation, whereas  $p=2$  leads to the notion of quadratic variation.

In practice, having a sample of length  $N+1$ :  $\{X_i, i=0, \dots, N\}$ , one calculates sample  $p$ -variation taking differences between every  $m$ th element of the data,

$$V_m^{(p)} = \sum_{k=0}^{N/m-1} |X_{(k+1)m} - X_{km}|^p, \quad (8)$$

see Figs. 3–6. Note also the essential difference between increments of  $X(t)$  in Eqs. (3) and (8).

One can show that for data from an  $H$ -self-similar process with stationary increments and finite moments  $V_m^{(p)} \sim m^{Hp-1}$ . In particular, this implies that in the case of FBM for  $p > 1/H$  sample  $p$ -variation is an increasing function of  $m$  (it tends to zero as  $m$  gets smaller), whereas for  $p < 1/H$  it is a decreasing function of  $m$  (it diverges to infinity when  $m$  gets smaller). For a FLSM the situation differs and depends on whether  $d$  is positive or negative. It appears that the sample  $p$ -variation is always a decreasing function with respect to  $m$  when  $d < 0$ . If  $d > 0$ , the situation is the same as in the finite moments case: if  $p > 1/H$ , then sample  $p$ -variation is an in-

creasing function of  $m$ , if  $p < 1/H$  it is a decreasing function of  $m$ .

This suggests a new  $p$ -variation dynamics test for checking both whether a given sample follows the self-similar dynamics and, in the subdiffusion case, distinguishing between a FBM (a light-tailed model) and a FLSM (a heavy-tailed

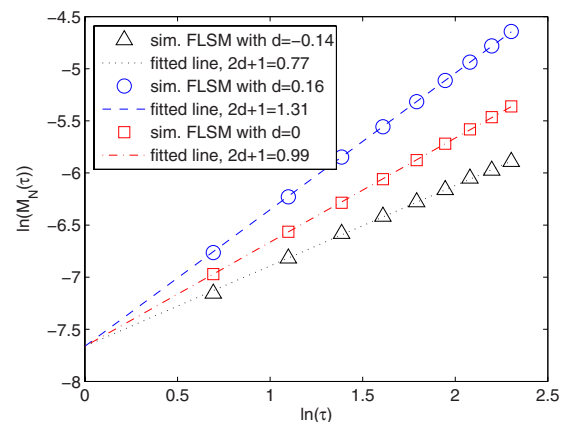


FIG. 2. (Color online) Sample MSD for a simulated trajectory from the FLSM with  $H=0.4$  and  $\alpha=1.85$  (black triangles)—subdiffusion case, a simulated trajectory from the FLSM with  $H=0.7$  and  $\alpha=1.85$  (blue circles)—superdiffusion case, and a simulated trajectory from the LSM with  $\alpha=1.85$  and  $H=1/\alpha$  (red squares)—diffusion case in double logarithmic scale. Estimated exponents equal 0.77 (corresponding black dotted line), 1.31 (blue dashed line), and 0.99 (red dash-dot line), respectively.

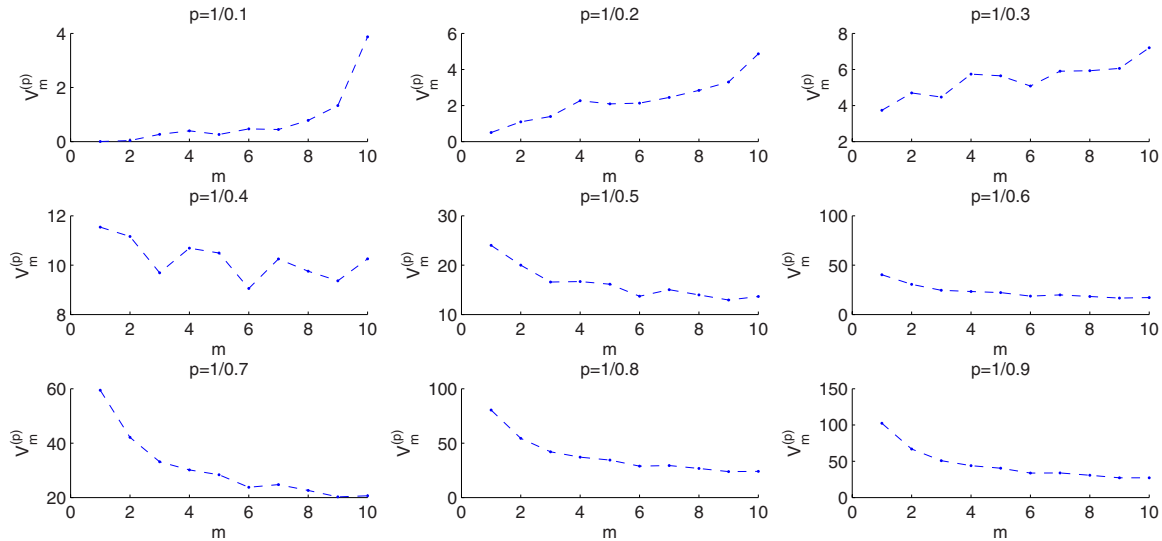


FIG. 3. (Color online) Sample  $p$ -variation for  $m=1,2,\dots,10$ ,  $H=0.1,0.2,\dots,0.9$  for a simulated trajectory from the FBM with  $H=0.4$  (the subdiffusion case). We observe that in the first three panels, sample  $1/H$ -variation increases, it stabilizes in the fourth panel (corresponding to  $H=0.4$ ), and it decreases in the subsequent panels.

model). For a self-similar model in the superdiffusion case, sample  $p$ -variation as a function of  $m$  should be monotonic and change its behavior from an increasing function to a decreasing one for some  $p=1/H$ ,  $0 < H < 1$ . In the subdiffusion case, light-tailed and heavy-tailed (power-law) dynamics differ.

(i) If the underlying model is a FBM, then sample  $p$ -variation should behave exactly as in the superdiffusion case, namely change its monotonic character from a decreasing to an increasing one for some  $p=1/H$ ,  $0 < H < 1$ .

(ii) If the underlying model is a FLSM, then sample  $p$ -variation as a function of  $m$  should be a decreasing function for all  $p=1/H$ ,  $0 < H < 1$  (in practice, for simulated samples from a FLSM one can observe that for large  $p$  the function has a quite chaotic character for moderate sample sizes).

In Figs. 3–6 we illustrate the behavior of sample  $p$ -variation for sub- and superdiffusion cases for both FBM and FLSM. The simulated samples are of length  $2^{10}$  resembling the situation of the biological data studied in [9]. In the superdiffusion case (Figs. 4 and 6), sample  $p$ -variation as a function of  $m$  is monotonic and changes its behavior from an increasing function to a decreasing one for some  $p=1/H$ ,  $0 < H < 1$  for both FBM and FLSM.

In the subdiffusion case (Figs. 3 and 5)  $p$ -variation dynamics test allows to distinguish between a FBM (a light-tailed model) and a FLSM (a heavy-tailed model). If the underlying model is a FBM, then sample  $p$ -variation behaves exactly as in the superdiffusion case, namely, changes its monotonic character from a decreasing to an increasing one for some  $p=1/H$ ,  $0 < H < 1$ . The behavior within a FLSM model is different, sample  $p$ -variation as a function of  $m$

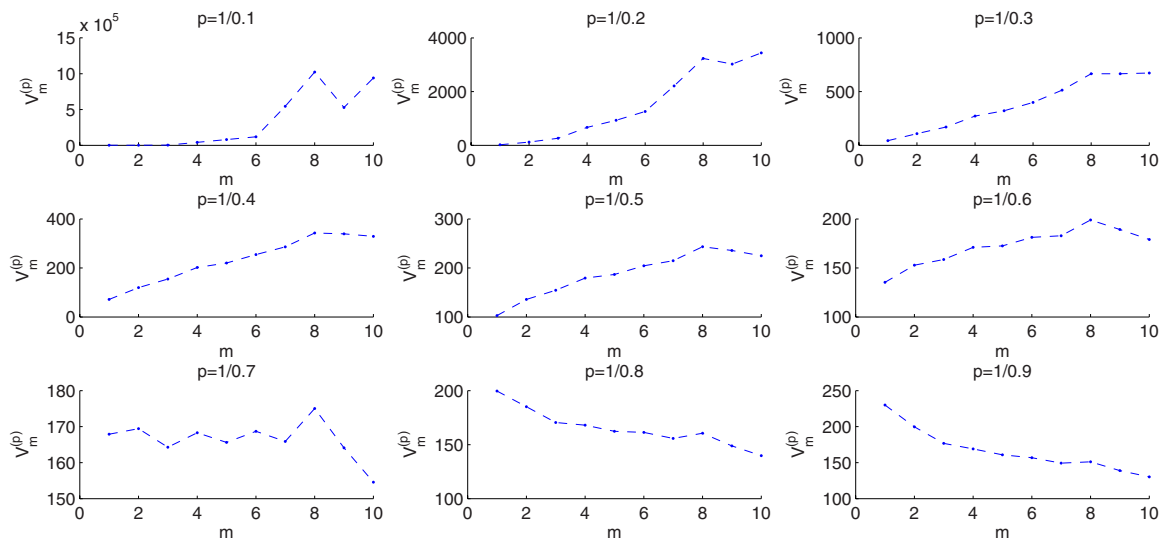


FIG. 4. (Color online) Sample  $p$ -variation for  $m=1,2,\dots,10$ ,  $H=0.1,0.2,\dots,0.9$  for a simulated trajectory from the FBM with  $H=0.7$  (the superdiffusion case). We observe that in the first six panels, sample  $1/H$ -variation increases, it stabilizes in the seventh panel (corresponding to  $H=0.7$ ), and it decreases in the subsequent panels.

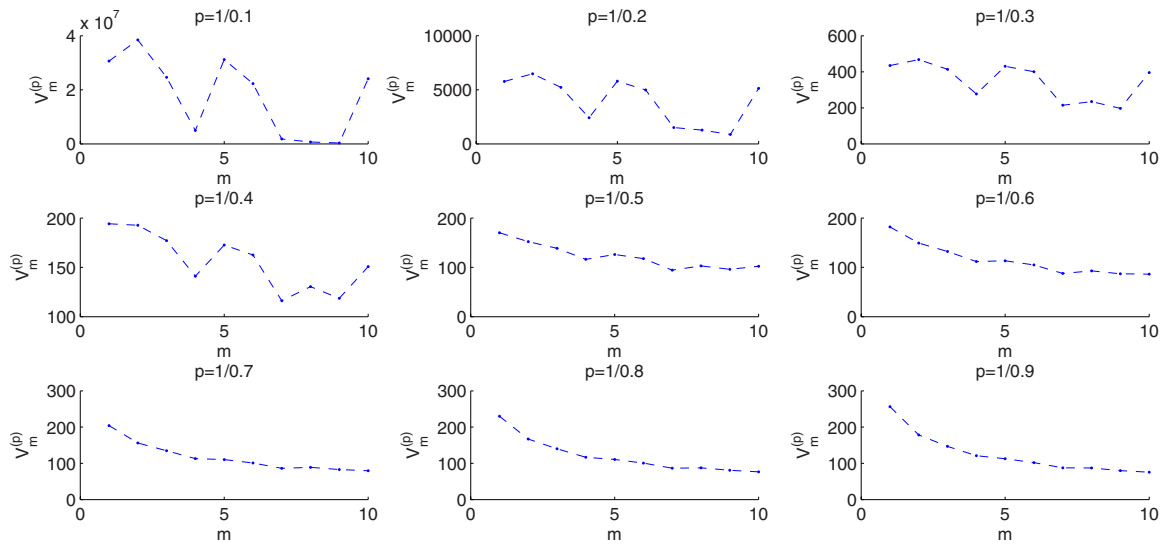


FIG. 5. (Color online) Sample  $p$ -variation for  $m=1,2,\dots,10$ ,  $H=0.1,0.2,\dots,0.9$  for a simulated trajectory from the FLSM with  $H=0.4$  and  $\alpha=1.85$  (the subdiffusion case). We observe that in the first three panels, sample  $1/H$ -variation does not show any clear trend, and it decreases in the subsequent panels.

should be a decreasing function for all  $p=1/H$ ,  $0 < H < 1$ . However, we can observe in Fig. 5, that for simulated time series from a FLSM, for large  $p$ , the function has a quite chaotic character for such a moderate sample size.

IV. EMPIRICAL DATA

We illustrate our findings on the data of Golding and Cox describing the motion of individual fluorescently labeled mRNA molecules inside live *E. coli* cells [9]. The data clearly follows the subdiffusive character and consists of 27 two-dimensional trajectories. In [7] two distinct models were analyzed for the underlying dynamics, namely FBM and CTRW. The main conclusion of the paper was a suggestion

that FBM can be considered as a possible model for the data. This was done on the basis of the calculation of sample  $p$ -variation for two values of  $p$ :  $p=2$  and  $p=1/0.35$  (0.35 was the value of the Hurst exponent taken from [9]). Here, we show that FLSM is a much better model, at least for some of the trajectories, which is justified by the studies of the self-similarity parameter, stability index and both sample MSD and sample  $p$ -variation. We illustrate the fit of the FLSM model to the  $y$ -coordinate of the longest trajectory of 1600 points and show it is a subdiffusive one, since  $d=H-1/\alpha < 0$ .

In order to check self-similarity of the data we used several estimation procedures of the Hurst exponent  $H$ , namely, absolute value, FIRT and variance of residuals (DFA) methods [36,37]. The results for  $H$  varied around 0.4. To estimate

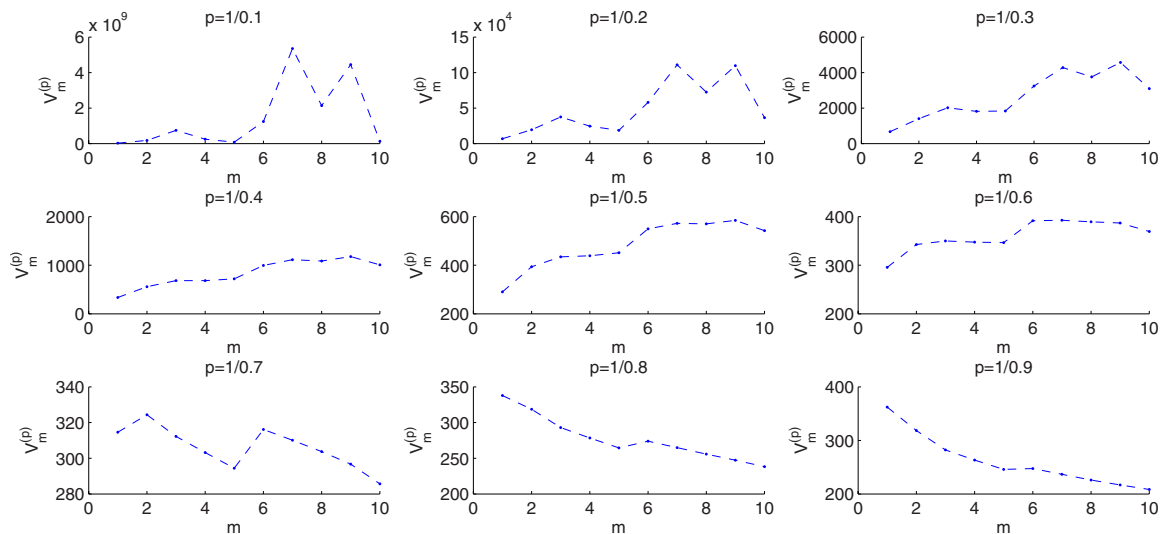


FIG. 6. (Color online) Sample  $p$ -variation for  $m=1,2,\dots,10$ ,  $H=0.1,0.2,\dots,0.9$  for a simulated trajectory from the FLSM with  $H=0.7$  and  $\alpha=1.85$  (the superdiffusion case). We observe that in the first six panels, sample  $1/H$ -variation increases, it stabilizes in the seventh panel (corresponding to  $H=0.7$ ), and it decreases in the subsequent panels.

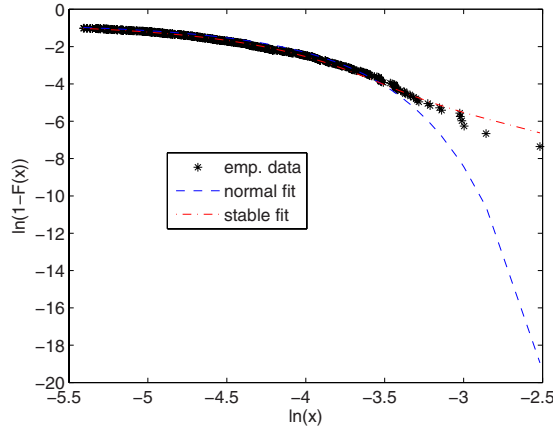


FIG. 7. (Color online) Tails of the empirical [9] (black asterisks), fitted normal (blue dashed line) and fitted Lévy stable (red dash-dot line) distribution functions in double logarithmic scale. Here  $x$  denotes values of the increments of the empirical process.

the stability index we employed a regression-type estimator, which is regarded as both accurate and fast [38]. The estimated stability index  $\alpha=1.85$ . To check the hypothesis of stability, we implemented following statistical tests: Kolmogorov-Smirnov, Kuiper, Cramer-von-Mises, Watson, and Anderson-Darling [39,40]. The calculated  $p$ -values for the considered tests were: 0.816, 0.793, 0.766, 0.709, 0.416, respectively. Such high  $p$ -values indicate the Lévy stable fit is very good. Applying the same procedure, we verified the hypothesis of normality, only the maximum likelihood method was used to estimate parameters of the Gaussian distribution. The calculated  $p$ -values for all considered tests were lower than 0.001, clearly indicating that a normal distribution hypothesis should be definitely rejected for the data. Both the Lévy stable and normal fits are illustrated in Fig. 7, where tails of the fitted and empirical distribution functions are depicted in the log-log scale.

Next, we calculated sample MSD for the data and for sample trajectories of both the fitted FBM and FLSM. In Fig. 8 we present the results. It appears that the estimated diffusion exponent for the data equals 0.65. Similar values are reproduced when simulating FLSM with  $H=0.4$  and  $\alpha=1.85$ , and not by simulating FBM with the estimated Hurst exponent  $H=0.4$ . Finally, we plotted sample  $p$ -variation with respect to  $m$  for  $p=1/H$ , where  $H=0.1, 0.2, \dots, 0.9$  for the studied data and for simulated realizations of both the fitted FBM and FLSM, see Fig. 9. We can see that the behavior of the  $p$ -variation for the data is similar to that of the simulated FLSM but not the FBM. Namely, the function does not show any clear trend for large  $p$  (equivalently, for small  $H$ ) and is decreasing with respect to  $m$  otherwise, whereas simulated trajectories of FBM produce increasing functions of  $m$  for  $p > 1/0.4$ , become flat around the value  $p=1/0.4$ , and for  $p < 1/0.4$  they result in decreasing functions.

## V. CONCLUSIONS

Our main finding is that the sample (time average) MSD is well defined for  $H$ -self-similar Lévy  $\alpha$ -stable processes for

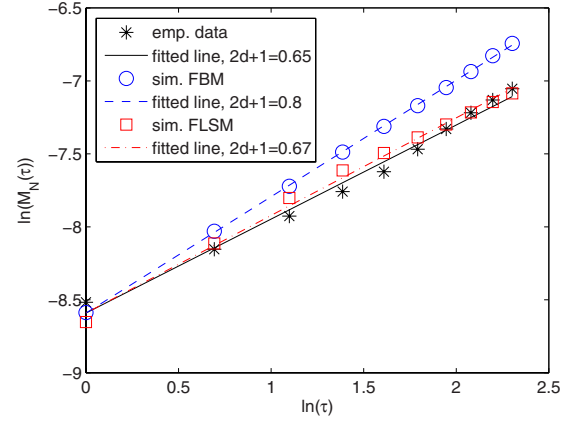


FIG. 8. (Color online) Sample MSD for the analyzed data (black asterisks), a simulated trajectory from the FBM with  $H=0.4$  (blue circles), and a simulated trajectory from the FLSM with  $H=0.4$  and  $\alpha=1.85$  (red squares) in double logarithmic scale. Estimated exponents equal 0.65 (corresponding black solid line), 0.8 (blue dashed line), and 0.67 (red dash-dot line), respectively.

$\alpha < 2$  and their diffusion character is fully controlled by the memory parameter  $d$ , see Eq. (4). Negative dependence corresponds to the subdiffusion case, whereas long-range dependence relates to the superdiffusion case. Hence a FLSM for  $d < 0$  can serve also as an example of subdiffusive dynamics.

We sum up now the presented results concerning the sample MSD:

(i) No  $\alpha$ -stable data for  $\alpha < 2$  can be subdiffusive in the traditional (ensemble) MSD sense since their second moment always diverges. Therefore, such data are classified as superdiffusive.

(ii) Hence in order to properly categorize the Golding and Cox experimental results (some of their data are 0.4-self-similar and 1.85-stable, which was statistically checked in this paper), we are forced to replace MSD with sample MSD, which allows a wider categorization of subdiffusion.

(iii) For FLSM we have: ensemble  $MSD(\tau) = \infty$ , whereas, as we proved, sample  $M_N(\tau)$  is proportional to  $\tau^{2d+1}$ .

(iv) The diffusion type is determined now by the memory parameter  $d$  which combines both the self-similarity parameter  $H$  and stability index  $\alpha$ .

(v) Sample MSD for finite second moment processes returns the same values as the traditional MSD, e.g., for the fractional Brownian motion  $M_N(\tau)$  is proportional to  $\tau^{2(H-1/2)+1} = \tau^{2H}$ .

(vi) Therefore, we claim that the sample MSD is a proper measure for categorization of anomalous diffusion in Gaussian and non-Gaussian cases and is closer to experimental data analysis.

In contrast to [7], we also described the dynamics of the sample  $p$ -variation for general Lévy stable processes, in particular, for a FBM and a FLSM. As a consequence, we constructed a new test which allows to check whether the dynamics underlying the data has a self-similar character and distinguish between two types of subdiffusive dynamics: FBM and FLSM. Finally, we showed that some of the bacterial cytoplasm data [9] can be modeled by a FLSM with  $d < 0$ . This was done employing various statistical tests, in-

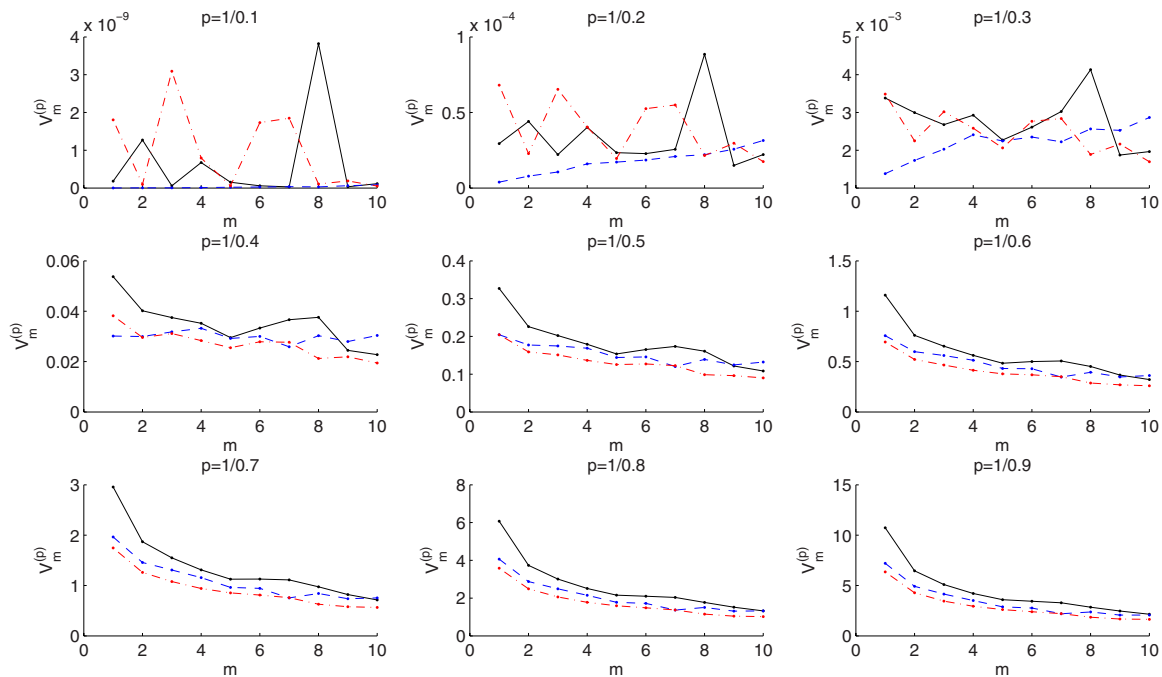


FIG. 9. (Color online) Sample  $p$ -variation for  $m=1, 2, \dots, 10$ ,  $H=0.1, 0.2, \dots, 0.9$  for the analyzed data (black solid line), a simulated trajectory from the FBM with  $H=0.4$  (blue dashed line), and a simulated trajectory from the FLSM with  $H=0.4$  and  $\alpha=1.85$  (red dash-dot line). We observe that for FBM, in the first three panels, sample  $1/H$ -variation increases, it stabilizes in the fourth panel (corresponding to  $H=0.4$ ), and it decreases in the subsequent panels. In contrast, in the cases of both analyzed data and FLSM, in the first two panels, sample  $1/H$ -variation does not show any clear trend, and it decreases in the subsequent panels.

roduced notion of sample MSD, and sample  $p$ -variation.

Let us also note that we have observed a similar effect for the data describing the epidermal growth factor receptor labeled with quantum dots in the plasma membrane of live cells presented in [5]. Nevertheless, we would like to warn the readers that one cannot rush into conclusions about the data, at least not until longer experiments are made. Therefore, we encourage experimentalists to make longer measurements with more trajectories, and with higher resolution. We hope that proposed in this paper statistical methodology will

be useful in determining rigorously the appropriate stochastic model behind the data.

### ACKNOWLEDGMENTS

The authors would like to thank Ido Golding and Arnaud Serge for providing the empirical data, and Eli Barkai, Joseph Klafter and Marcin Magdziarz for fruitful discussions. This work was partly supported by KBN grant.

[1] X. S. Xie and H. P. Lu, *J. Bio. Chem.* **274**, 15967 (1999).  
 [2] S. Weiss, *Nat. Struct. Biol.* **7**, 724 (2000).  
 [3] W. Moerner, *J. Phys. Chem. B* **106**, 910 (2002).  
 [4] S. C. Kou, V. S. Xie, and J. S. Lin, *J. R. Stat. Soc., Ser. C, Appl. Stat.* **54**, 469 (2005).  
 [5] A. Serge, N. Bertaux, H. Rigneault, and D. Marquet, *Nat. Methods* **5**, 687 (2008).  
 [6] I. Bronstein, Y. Israel, E. Kepten, S. Mai, Y. Shav-Tal, E. Barkai, and Y. Garini, *Phys. Rev. Lett.* **103**, 018102 (2009).  
 [7] M. Magdziarz, A. Weron, K. Burnecki, and J. Klafter, *Phys. Rev. Lett.* **103**, 180602 (2009).  
 [8] G. Guigas, C. Kalla, and M. Weiss, *Biophys. J.* **93**, 316 (2007).  
 [9] I. Golding and E. C. Cox, *Phys. Rev. Lett.* **96**, 098102 (2006).  
 [10] R. Metzler and J. Klafter, *Phys. Rep.* **339**, 1 (2000).  
 [11] R. Metzler and J. Klafter, *J. Phys. A* **37**, R161 (2004).  
 [12] M. Kotulska, *Biophys. J.* **92**, 2412 (2007).  
 [13] A. Caspi, R. Granek, and M. Elbaum, *Phys. Rev. Lett.* **85**, 5655 (2000).  
 [14] A. Lubelski, I. M. Sokolov, and J. Klafter, *Phys. Rev. Lett.* **100**, 250602 (2008).  
 [15] Y. He, S. Burov, R. Metzler, and E. Barkai, *Phys. Rev. Lett.* **101**, 058101 (2008).  
 [16] B. B. Mandelbrot and J. W. Van Ness, *SIAM Rev.* **10**, 422 (1968).  
 [17] M. Magdziarz, *Stoch. Models* **26**, 256 (2010).  
 [18] A. Weron and M. Magdziarz, *EPL* **86**, 60010 (2009).  
 [19] E. Lutz, *Phys. Rev. E* **64**, 051106 (2001).  
 [20] A. Weron, K. Burnecki, Sz. Mercik, and K. Weron, *Phys. Rev. E* **71**, 016113 (2005).  
 [21] S. C. Kou and X. S. Xie, *Phys. Rev. Lett.* **93**, 180603 (2004).  
 [22] W. Deng and E. Barkai, *Phys. Rev. E* **79**, 011112 (2009).

- [23] J. H. Jeon and R. Metzler, *Phys. Rev. E* **81**, 021103 (2010).
- [24] N. W. Watkins, D. Credgington, R. Sanchez, S. J. Rosenberg, and S. C. Chapman, *Phys. Rev. E* **79**, 041124 (2009).
- [25] A. Janicki and A. Weron, *A Simulation and Chaotic Behaviour of  $\alpha$ -Stable Stochastic Processes* (Marcel Dekker Inc., New York, 1994).
- [26] G. Samorodnitsky and M. S. Taqqu, *Stable Non-Gaussian Random Processes* (Chapman & Hall, New York, 1994).
- [27] S. Stoev and M. S. Taqqu, *Fractals* **12**, 95 (2004).
- [28] P. S. Kokoszka and M. S. Taqqu, *Ann. Stat.* **24**, 1880 (1996).
- [29] R. McGill, J. W. Tukey, and W. A. Larsen, *Am. Stat.* **32**, 12 (1978).
- [30] P. F. Velleman and D. C. Hoaglin, *Applications, Basics, and Computing of Exploratory Data Analysis* (Duxbury Press, Boston, 1981).
- [31] B. Dybiec and E. Gudowska-Nowak, *Phys. Rev. E* **80**, 061122 (2009).
- [32] A. Zoia, A. Rosso, and S. N. Majumdar, *Phys. Rev. Lett.* **102**, 120602 (2009).
- [33] S. N. Majumdar, A. Rosso, and A. Zoia, *Phys. Rev. Lett.* **104**, 020602 (2010).
- [34] M. Magdziarz and J. Klafter, *Phys. Rev. E* **82**, 011129 (2010).
- [35] T. F. Chan and J. Shen, *Image Processing. Variational, PDE, Wavelet and Stochastic Methods* (SIAM, Philadelphia, 2005).
- [36] S. Stoev, V. Pipiras, and M. S. Taqqu, *Signal Process.* **82**, 1873 (2002).
- [37] M. S. Taqqu and V. Teverovsky, in *A Practical Guide To Heavy Tails: Statistical Techniques and Applications*, edited by R. J. Adler *et al.* (Birkhäuser, Boston, 1998).
- [38] I. A. Koutrouvelis, *J. Am. Stat. Assoc.* **75**, 918 (1980).
- [39] R. B. D'Agostino and M. A. Stephens, *Goodness-of-Fit Techniques* (Marcel Dekker, New York, 1986).
- [40] K. Burnecki, A. Misiorek, and R. Weron, in *Statistical Tools for Finance and Insurance*, edited by P. Cizek *et al.* (Springer, Berlin, 2005).